Special Issue of the 8th International Advances in Applied Physics and Materials Science Congress (APMAS 2018)

The Effects of Austempering Heat Treatment on the Mechanical Properties of Heavy Vehicles Camshaft made of Different Analysis Ductile Cast Iron

B. Karaca[a,*] and M. Şimşir[b]

[a]ESTAŞ Eksantrik San. ve Tic. A.Ş., 58060 Sivas, Turkey

[b]Cumhuriyet University, Department of Metallurgy and Materials Eng., 58100 Sivas, Turkey

The aim of this study was to investigate the effect of the austempering treatment applied on ductile graphite cast iron with different chemical composition; microstructure, hardness, tensile strength and wear resistance. For this purpose sand mold casting models of camshafts were prepared and casting simulation was carried out with the NOVACAST program. The casting quality of camshafts and production process was optimized. For nodulizing process, Fe–Si–Mg alloy has been used and Fe–Si–Ba–Ca–Al alloy has been used for inoculation process. The casting has been done 1430 °C and the pouring time in 15 s. In different analyzes, a cast camshaft subjected to a 90 min austenitizing process at 900 °C under a mill vacuum furnace. The austenitized cam shafts have been quenched into the molten salt bath (50% KNO_3 + 50% $NaNO_3$) at 260 °C temperature, held for 30, 60, 90, 120, 150, 180 and 210 min and then cooled in air. Microstructures analysis of cam shafts have been examined by optical microscope and scanning electron microscopy (SEM), mechanical tests (hardness, tensile tests and wear tests) have been performed. Results show that austempering heat treatment increases the tensile strength of cam shaft as-cast condition. In this study, the tensile strength values of the austempered structure, camshaft core which has been formed in 120 minute duration which has the combination of excellent strength and ductility, have been brought from the level of 711.08 MPa to 1424.28 MPa.

DOI: 10.12693/APhysPolA.135.804

PACS/topics: casting, austempering, tensile properties, wear properties, SEM

1. Introduction

The production of camshafts used in engines is carried out with the casting and machining techniques. Today, camshafts are produced from gray, nodular graphite cast iron, because of many advantages, or machining of steel [1]. The use of spheroidal graphite cast iron provides parts with high tensile strength, high ductility, high wear resistance, low melting temperature, and easy and low cost production [2].

Chemical composition is an important factor in the production of spheroidal graphite cast irons. The microstructure of spherical graphite cast iron should be nonporous, exhibit good sphericity and without carbides between cells. The mechanical properties of spheroidal graphite cast irons are directly related to the microstructure of the material, and the microstructure of this material may be fully perlitic, ferritic/perlitic or fully ferritic. The main determinant of this structure is the chemical composition of the material [3].

The choice of composition and raw materials for spheroidal graphite cast iron, the elimination of elements that produce non-spherical graphite, carbides and inclusions that negatively affect casting quality should be considered. When deciding on the alloying requirements, the type, intensity, and slice thickness of the austempering cooling should also be taken into account [4, 5].

Austempering heat treatment may be implemented to spherical graphite cast iron. As researches on austempered spheroidal graphite cast iron become more and more popular, the field of its exploitation also increases. Austempered spherical graphite cast irons becomes to be the replacement of casting or forging steels in the automotive industry [6, 7].

As the size of parts made of spherical graphite cast iron grows, it is difficult to obtain good quality of castings suitable for austempering. The bigger the parts are, the lower is the cooling rate, so the number of graphite sphere decreases and micro-shrinkage, porosity, and deterioration of graphite sphericity and eutectic carburetion and segregation of alloying elements such as Mn and Mo may occur [8].

The spherical graphite cast iron should contain high amounts of alloying elements, necessary for the completion of the austempering process. Higher amounts of alloying elements increase the possibility of segregation [9, 10].

The aim of this study is to investigate the effects of austempering on microstructure and mechanical properties of heavy vehicles camshaft.

2. Materials and equipments

In order to eliminate possible errors, of sand casting models in the NovaCast casting simulation program by 3D solid modeling the feeders were simulated the liquid metal filling (Fig. 1) and shrinkage before the production of ductile iron camshaft.

*corresponding author; e-mail: bahadir.karaca@estas.com.tr

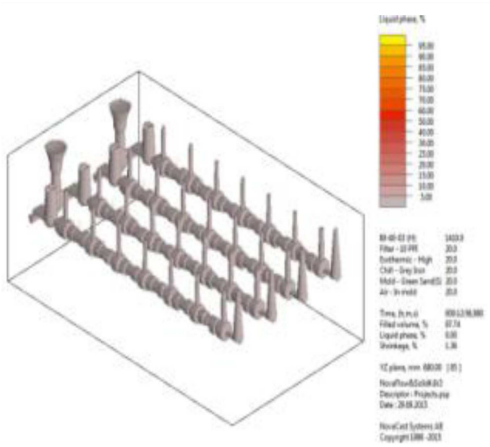

Fig. 1. Casting simulation.

Sand molds to be used in the camshaft casting were prepared. Melting the metal of three different chemical compositins were conducted in induction furnaces. The chemical composition was analyzed by spectrometer and Atas termal analysis equipment. Table I shows the chemical compositions of cast iron used in camshaft production.

Nodulizing process was done in the treatment crucible at the temperature of 1550–1570 °C. Fe–Si–Mg alloy was used for nodulizing treatment. While liquid metal was poured into casting crucible, inoculation process was done by adding Fe–Si–Ba–Ca–Al alloy. Casting process was completed in 15 s and at the temperature of about 1430 °C by controlling laser type thermocouple. By this way, camshaft and tensile samples (Y blocks) were casted by sand mold casting method.

Chemical composition of casting camshaft material. TABLE I

Material	C	Si	Mn	P	S	Mg	Cr	Ni	Mo	Cu	Sn	Fe
1 Nu	3.59	2.49	0.286	0.032	0.022	0.038	0.082	0.057	0.021	0.045	0.003	bal.
2 Nu	3.67	2.46	0.166	0.031	0.023	0.047	0.050	1.038	0.209	0.546	0.03	bal.
3 Nu	3.65	2.44	0.313	0.027	0.022	0.042	0.048	1.027	0.200	0.532	0.002	bal.

Remaining sands on the surface of camshafts and Y blocks has been cleaned by sand blasting device. The runners and risers of camshafts and Y blocks were separated by cutting and their surfaces were ground on CNC machines. Tensile test samples were produced from Y blocks according to ASTM A597 standard (Fig. 2).

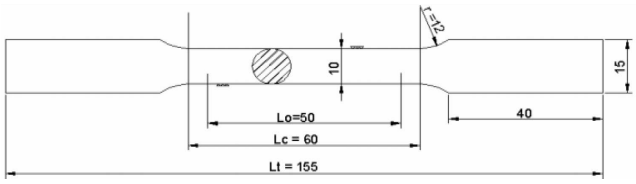

Fig. 2. ASTM A597 standard tensile sample 2D technical drawings.

In the austempering heat treatments, cabin type electric furnace is used. It attains the temperature up to 1100 °C and assures atmosphere and temperature control. Camshafts of 3 different chemical compositions were austenitized at 900 °C, 90 min, austempered rapidly in salt bath (50% KNO_3 + 50% $NaNO_3$) at 260 °C for 30, 60, 90, 120, 150, 180 and 210 min. After that, camshafts were air cooled to room temperature.

Heat treated camshafts samples were prepared for microstructure investigation by standard metallographic methods (mounting, grinding, polishing) and then etching process was applied by using 2% nital solution. The microstructure of the camshaft was examined under a Nikon MA200 optical microscopy and analyzed by Clemex Vision Lite image analysis software. The nodularity rate, nodule size and number, graphite volume percentage, ferrite and pearlite rate were measured.

Hardness of core sections of camshafts as-casted and austempered were measured applying 750 kgf load in terms of the Brinell hardness by Instron Wolpert hardness device. Hardness test was measured five times for different sections.

Tensile test machine called ALSA with 20 tons load was used for tension test. Tensile strength, yield strength and the elongation were determined. Tension test were conducted three times and average values of tensile properties were given and then the fracture surfaces of each sample were examined by SEM.

For wear tests, wear test sample were prepared by cutting bits from cam sections of the camshafts under as-casted and heat treated conditions. UTS T10/20 brand pin-on disc type test apparatus (tribometer) was used for wear test. Wear test was conducted in accordance with ASTM G99-05 standard, for various loads, constant distance and at constant rpm. Then, weight loss was measured by sensitive balance. Because of ASTM G99-05 standard is based on the measurement of wear volume, wear on ball bearing was calculated by using mathematical relationship and indirectly determined volumetric loss.

At the room temperature, under load of 30 N, rotation speed of 300 rpm, at 500 m distance, wear test with 100Cr6 material 5 mm in diameter was performed

3. Results and discussion

The results of the image analysis obtained by Clemex Vision Lite program are given in Table II. As seen in the Table: nodularity percentage, nodules number and size, graphite, ferrite and pearlite volume ratio values are close to that in GGG80 cast iron standard.

TABLE II

Microstructural analysis results.

Material	Nodularity [%]	Nodule number [mm^2]	Size of nodule [μm]	Graphite volume [%]	Ferrite volume [%]	Perlite volume [%]
1 Nu (unalloyed)	79	221	22.27	14.33	29.18	56.49
2 Nu (low Mn/Cu-Ni alloyed)	87	268	17.63	9.71	31.39	58.90
3 Nu (high Mn/Cu-Ni alloyed)	91	319	14.13	7.49	33.02	59.49

The data confirm, that the method implemented to the camshaft production is correct and reliable. A linear increase in pearlite volume is obtained, when the amount of Ni and Cu grows. Accordingly, with increasing of Mn amount, the increase is also observed. Ni has slightly bigger influence in sphere number, distribution and volume ratios.

The microstructure of camshafts with three different chemical compositions is given in Fig. 3a–c. The microstructure is typical for graphite cast iron casts structure. The spheroidized graphite nodules contain ferrite-converted particles, which are carbonized around the graphite nodules, and a perlitic matrix outside them. The increasing of the number of graphite spheres increases the ferrite volume ratio. So called bulls eyes, i.e. ferrite structures close to generally graphite spheres and perlite are seen in different parts.

The changes in microstructure depending on the austempering period are shown in Figs. 4–6. In all the austempered samples (Fig. 4a–g), the microstructure was made up austenite and unconverted austenite, depending on the duration of the process.

After the etching in 2% nital ferrite is seen dark, high-carbon austenite light-colored and untransformed austenite appear as light-colored large areas (Fig. 4a–g). The austempering heat treatment at 260 °C leads to the precipitation of the austenite into the ferrite. After the processing, ferrit and the transformed austenite amounts increase on the cost of untransformed austenite amount, dependent on processing time (Figs. 4–6a–d). In general, the alloying elements slow down the transformation speed and keep the presence of untransformed austenite high even though the austempering progress time increases. As the austempering period increases behind the treatment interval, the number of spheres decreases (Figs. 4–6d–g) and the sphere sizes increases accordingly. Higher number of spheres increases the transformation speed and reduces the formation of boundaries. The formation of carbides is linked to Mn content, the austempering time and the segregation of cells (Fig. 6d–g).

The core of the camshaft cools slower than its surface, and therefore it is softer, as measured with the Brinell hardness. The changes in the hardness of the samples in respect to the casting conditions and the austempering time are given in Table III. Increase in Ni and Cu amount in the casted sample increases the amount of perlite in the phase structure and accordingly an increase in the hardness is observed. This is due to the increase in the amount of carbon dissolved in the austenite matrix. Nevertheless it is visible, that the changes of the hardness valuee of the austempered samples is not essential. The increase in the austempering period decreases the hardness of all samples. In addition, degradation of sphericity deteriorates the mechanical properties.

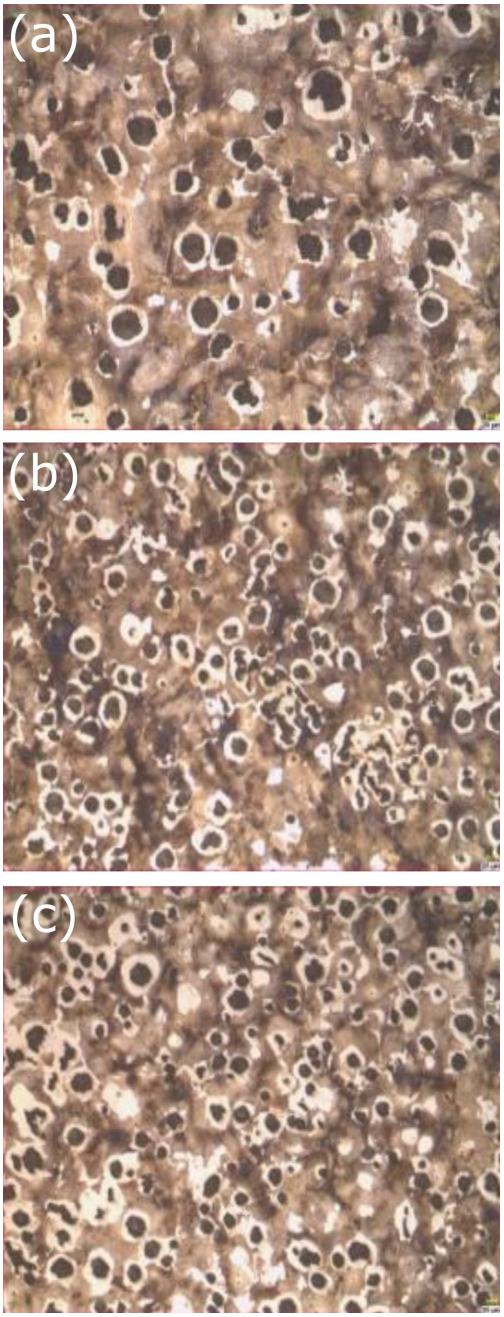

Fig. 3. The microstructure of the cast camshaft, 100×; (a) 1 Nu, (b) 2 Nu, (c) 3 Nu.

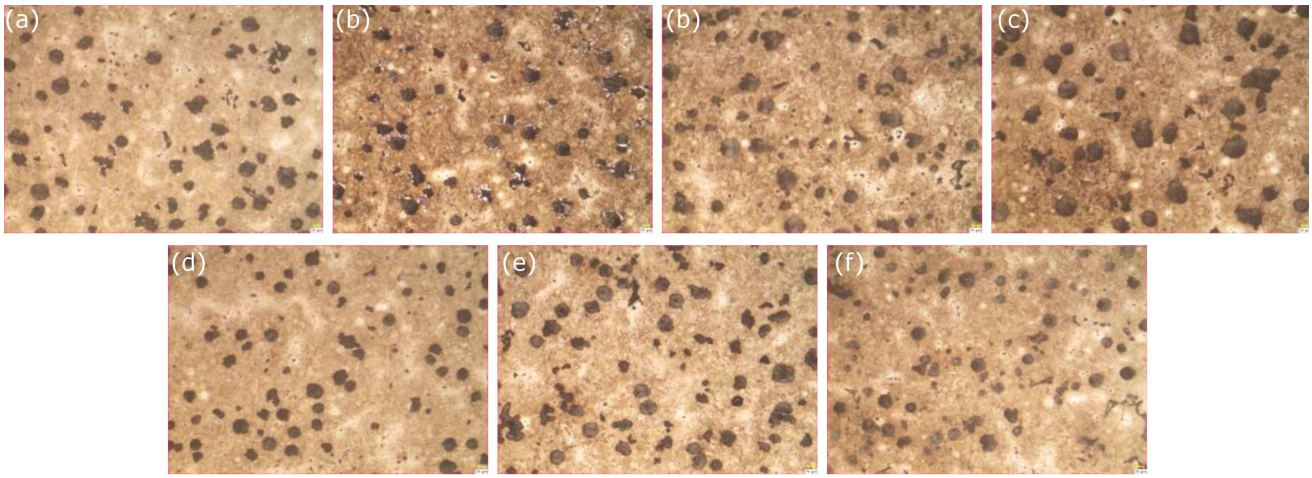

Fig. 4. Microstructure of the austempered camshaft (chemical composition number 1), 100×; (a) 30 min, (b) 60 min, (c) 90 min, (d) 120 min, (e) 150 min, (f) 180 min, (g) 210 min.

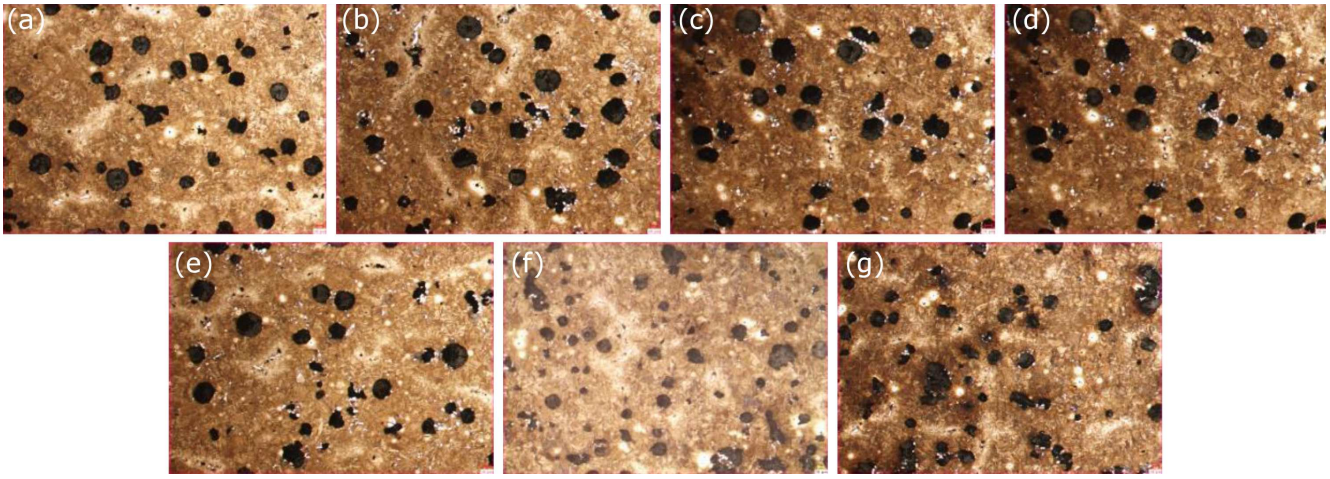

Fig. 5. Microstructure of austempered camshaft (chemical composition number 2), 100×; (a) 30 min, (b) 60 min, (c) 90 min, (d) 120 min, (e) 150 min, (f) 180 min, (g) 210 min.

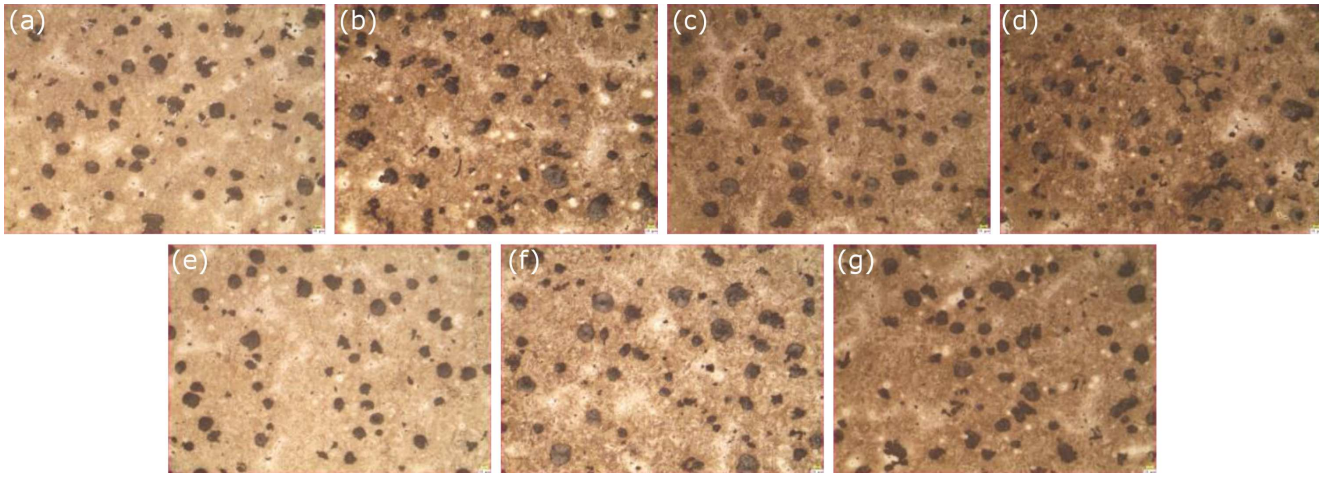

Fig. 6. Microstructure of austempered camshaft (chemical composition number 3), 100×; (a) 30 min, (b) 60 min, (c) 90 min, (d) 120 min, (e) 150 min, (f) 180 min, (g) 210 min.

TABLE III

Hardness analysis results [HB].

Material	as-cast	30 min aus.	60 min aus.	90 min aus.	120 min aus.	150 min aus.	180 min aus.	210 min aus.
1 Nu	202	444	468	384	373	361	356	350
2 Nu	211	451	444	397	380	365	354	348
3 Nu	221	463	489	410	389	378	362	357

TABLE IV

Tensile test results

Material	Tensile properties	as-cast	30 min aus.	60 min aus.	90 min aus.	120 min aus.	150 min aus.	180 min aus.	210 min aus.
1 Nu	yield strength [MPa]	334.48	526.25	556.65	613.19	605.14	591.22	584.63	526.24
	tensile strength [MPa]	469.94	995.28	1084.13	1281.21	1265.17	1214.24	1200.91	1158.63
	elongation [%]	8.30	4.67	3.40	2.90	2.76	2.83	2.89	3.16
2 Nu	yield strength [MPa]	438.54	546.93	580.85	615.39	634.44	597.77	590.41	564.56
	tensile strength [MPa]	691.42	1070.29	1150.73	1287.08	1338.73	1307.38	1293.86	1265.56
	elongation [%]	6.10	3.96	3.16	2.75	2.62	2.77	2.86	3.08
3 Nu	yield strength [MPa]	444.88	562.28	564.79	627.07	634.50	603.97	601.48	577.15
	tensile strength [MPa]	711.08	1104.33	1238.10	1346.20	1444.28	1324.80	1313.03	1275.18
	elongation [%]	5.20	3.26	2.93	2.66	2.57	2.64	2.80	2.99

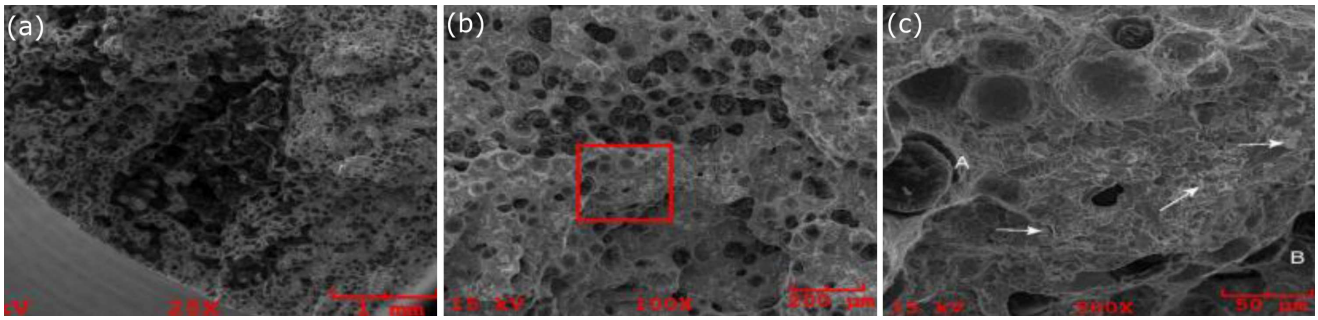

Fig. 7. Stretched as-cast sample with chemical composition number 3; SEM images of fracture surface of: (a) general fracture zone, (b) details of the central region, (c) details of the red framed region of (b).

Tensile tests were conducted three times for each sample and average values of tensile properties were calculated and submitted. Tensile test results are given in Table IV. It is observed, that the increase in Ni, Cu and Mn amount in the as-casted samples increases the amount of perlite in the final phase structure, resulting an increase in tensile values and a decrease in elongation value. When the tensile strength of all austempered samples was examined, the tensile strength increased with the increase in the number of spheres in the elapsed time until the completion of the phase transformation of the samples (working interval). The tensile strength decreases with the decrease in the number of spheres at the austempering period after the treatment interval. The full tensile strength of unalloyed samples was reached after 90 minutes, while the full tensile strength of samples with increased Ni and Cu contents was reached after 120 minutes of austempering. Alloying elements make carbon diffusion difficult and cause the formation of more stable carbon-rich austenite longer. When the process time surpasses certai limit, the austenite becomes too stable to subject transformation; martensite formation on the surface is prevented. It causes the tensile strength decrease between the 150th and the 210th minute. As the austempering time increases, an increase in the yield strength of the samples is observed, depending on the casting conditions. In the second stage of austempering, after the process interval, between the 150th and the 210th minute the flow resistance decreases.

Figure 7 shows three different views of the general fracture (break) region for the cast made of third mixture. It can be seen that a porous region is covered by a wide indentation-protruding region. Figure 7b shows the general image of fault and Fig. 7c shows the detail surrounded by red frame in Fig. 7b. In Fig. 7b the mixed fraction is seen. There are the nodules around the ductile fracture feature called "dimple rupture", separated by the ferrite matrix susceptible to the plastic deformation and the non-deformable nodules the in the housing. These nodules acts as perfect starting point of damages. The dispersed areas called "dimple" (see A, in Fig. 7c), which are resembling a patchwork, generate a cleavage like fractures that have brittle fracture type characteristic. The areas marked B in Fig. 7c are called "quasi-cleavage".

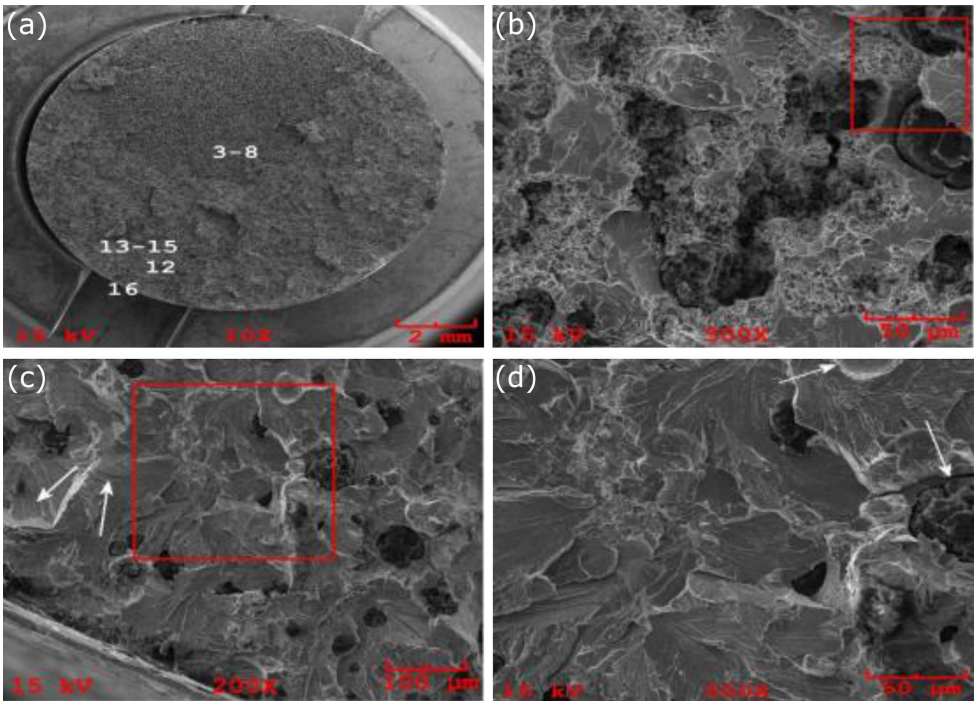

Fig. 8. Stretched, 120 min austempered tensile sample with chemical composition number 3; SEM images of fracture surface of: (a) general fracture zone, (b) details of the central region, (c) formation of "river pattern" and cleavage steps (white arrows) near the surface, (d) detail of the red framed region.

Wear test results

TABLE V

Material	Wear properties	as-cast	30 min aus.	60 min aus.	90 min aus.	120 min aus.	150 min aus.	180 min aus.	210 min aus.
1 Nu	loss of sample [mg]	1.0611	0.4409	0.4214	0.5221	0.5619	0.5928	0.6261	0.6523
	friction coefficient	0.6841	0.2940	0.3050	0.3110	0.3240	0.3320	0.3490	0.3530
2 Nu	loss of sample [mg]	0.9234	0.3675	0.3537	0.4832	0.5113	0.5489	0.5906	0.6105
	friction coefficient	0.6533	0.2890	0.2970	0.3020	0.3090	0.3130	0.3252	0.3390
3 Nu	loss of sample [mg]	0.8876	0.3392	0.3263	0.4591	0.4864	0.5112	0.5621	0.5899
	friction coefficient	0.6212	0.2670	0.2690	0.2710	0.2870	0.2990	0.3140	0.3210

A general fracture image of 120 minute austempered camshaft sample with chemical composition number 3 is given in Fig. 8. It exhibits a brittle fracture zone ranging from the top to the center. Figure 8b shows the detail of the cross section with central big brittle fracture. The nodule morphology is partly eccentric and the dense precipitate is seen in the matrix. In Fig. 8c the intense cleavage near the outer surface can be seen. White arrows indicate that the fracture proceeds in the cleavage steps. Details of the region surrounded by red frame in Fig. 8c can be seen in panel 8d. There is no ferritic area around the nodules and the interface acts as a crack starting region as shown by white arrows.

The results of wear tests conducted for 30 N load are given in Table V. It can be seen, that increasing the amount of Ni and Cu in the cast favors the perlite formation. The hardness increases and accordingly the wear decreases. The rate of abrasion is decreased for all austempered camshaft samples. The lowest pace of wear under the load of 30 N was found for the camshaft made of chemical composition number 3 and austempered for 120 min. The highest rate of wear of the bearing ball, that was used as an abrasive agent, was achieved for the as-cast camshaft samples under the load of 30 N, because the highest coefficient of friction observed in this test.

4. Conclusions

In this study, the effect of the austempering treatment applied on ductile graphite cast iron with different chemical analyzes microstructure, hardness, tensile strength, wear resistance were investigated. The following results were obtained:

1. When the microstructure of the the as-cast camshaft contains graphite nodules and ferritic-pearlitic matrix structure, austempered camshaft contains ausferrite (austenite + ferrite) microstructure.

2. Perlite volume ratio increases with the increase in Ni, Cu and Mn contents. Ni is more effective in the formation of perlite than Cu.
3. The amount of untransformed austenite decreases with the austempering time, while the amount of ferrite and high-carbon austenite increases.
4. The size of the sphere increases and the number of sphere per unit area decreases with the austempering time.
5. The addition of alloying elements in as-cast conditions increases the perlite volume ratio and the hardness.
6. Austempering process applied on GGG80 class nodular cast iron augments the core hardness value from 202 HB to 489 HB.
7. Austempered cast iron has 90–95% higher tensile strength than the as-cast camshaft. The maximum tensile strength was obtained for the camshaft having chemical composition 3, austenitized at 260 °C for 120 min. Similar results were obtained for yield strength. However, the elongation is decreased by austempering heat treatment.
8. In general, the addition of alloying elements increases the tensile strength due to the increase in the perlite volume ratio, while the elongation decreases. As the austempering time increases (up to the process range, 120 min), tensile strength and yield strength increase. Further sustaining of the process reverts this tendency.
9. The wear under the load of 30 N is the adhesive wear. A 60% increase in abrasion resistance can be achieved due to the addition of Ni and Cu and the austempering.
10. Perlite volume ratio, hardness, tensile and abrasion resistance of the composition number 3, enriched with Ni, Cu and some amount of Mn, is increased. The results are better than for other materials and the austemperability is more efficient.

References

[1] M.M. Elsayed, A.A. Megahed, K.M. Sadek, K.M. Abouelela, *Mater. Des.* **30**, 1866 (2009).

[2] N. Fatahalla, A. Abu el Ezz, M. Semeida, *Mater. Sci. Eng. A*, **504**, 81 (2009).

[3] A. Kiani-Rashid, D.V. Edmonds, *J. All. Comp.*, **477**, 391 (2009).

[4] L. Bartosiewicz, F.A. Alberts, I. Singh, *J. Mater. Eng. Perform.* **4**, 90 (1994).

[5] N. Bhople, S. Patil, M. Harne, S. Dhande, *Int. J. Innov. Res. Sci. Eng. Technol.* **5**, 1197 (2016).

[6] K. Narasimha-Murthy, S. Sampathkumaran, S. Seetharamu, *Wear* **267**, 1393 (2009).

[7] H. Santos, J. Seabre, A. Duarte, *Int. J. Cast Metals Res.* **15**, 117 (2002).

[8] C. Qing, M.Sc. Thesis, Institute of Mechanical Engineering, National Taiwan University, 2010.

[9] J. Serrallach, J. Lacaze, R. Suarez, A. Monzon, *Key Eng. Mater.* **457**, 361 (2011).

[10] A. Trudel, M. Gagné, *Canad. Metal. Quart.* **36**, 289 (1997).